# Structure and stacking-fault energy in metals Al, Pd, Pt, Ir, and Rh

J. Cai
*Department of Material Science, National University of Singapore, Singapore 119260*

F. Wang, C. Lu, and Y. Y. Wang
*Division of Computational Mechanics, Institute of High Performance Computing, The Capricorn, Science Park II, Singapore 117528*

(Received 23 December 2003; revised manuscript received 1 March 2004; published 10 June 2004)

The generalized stacking faults of Al, Pd, Pt, Ir, and Rh are investigated by a parametrized tight-binding potential. The stacking-fault energies (SFEs) are calculated to be in good agreement with experimental data, except for Al. More important, it is found that the SFE of Pt may be reduced by 14% by atom relaxation while the effect of atom relaxation on the SFEs of Al, Pd, Ir, and Rh are small. Thus, it is concluded that the effect of atom relaxation on SFE should be important, especially for an alloy system where radii difference between two constituting elements is large.

DOI: 10.1103/PhysRevB.69.224104 PACS number(s): 61.72.Nn, 71.15.Nc

## I. INTRODUCTION

The atom interaction potential is very important for simulating atom-scale microscopic structure and microscopic dynamic process in materials science. A pair potential model fails to simulate some basic properties of metal materials, such as surface, vacancy, elastic constants,[1] phase transition,[2] etc. A many-body potential model, based on the embedded-atom method,[1,2] has resolved the problems met by a pair potential model. However, a more rigorous challenge is found when the embedded-atom method is used to calculate stacking-fault energy (SFE). In a recent work, Zimmerman *et al.*[3] calculated generalized stacking-fault (GSF) energies of Al, Ni, and Cu by the embedded-atom method. They found that, as compared to experimental data, the SFEs and unstable SFEs were underestimated in most cases. (The unstable SFE refers to the lowest energy barrier encountered when one half of a crystal slips along the other one.[3]) At the same time Mehl *et al.*[4,5] developed a tight-binding (TB) potential to study SFE and unstable SFE of fcc metals. They made a comparison among the results by themselves, *ab initio* calculations, embedded-atom method calculations, and experimental data. They found that the results by themselves were in good agreement with the *ab initio* calculations or experimental data. This is impressive, since their tight-binding potential only fits to *ab initio* total energy and band structures of cubic metals. They also found that comparable accuracy with the embedded-atom method can be achieved only by fitting to the stacking-fault energy.[4,5] The tight-binding potential of Mehl *et al.*[4,5] reveals the promise to describe this type of issue. In their calculations, however, atom relaxation was not considered, except for the cases of unstable SFE of Au and Ir. In the works of Zimmerman *et al.*,[3] there were also no discussions about the relaxed GSF structures, although the effect of atom relaxation on GSF energies was considered.

The energy and structure of generalized stacking fault have strong effect on mechanical properties of materials.[5–8] Although they are closely related to the dynamic properties of dislocations, to our knowledge, little is known about the structure properties of GSF when atom-scale relaxation is considered. On the other hand, the effect of atom relaxation on SFE has been considered negligible without good reason.

In this work, we study the GSF structural properties of Al, Pd, Pt, Ir, and Rh using the TB potential[4] combined with a simulated annealing method.[9] In the following, a general theory and method about the TB potential are given first, then in Sec. III, the numerical results and discussions are presented, and finally, the conclusions are given.

## II. THEORY AND METHOD

The tight-binding potential of Mehl *et al.*[4] and a simulated annealing method[9] are used to relax the GSF structures of Al, Pd, Pt, Ir, and Rh. The potential model is developed from density-functional theory (DFT).[10] In the DFT, the total energy of a system of $N$ atoms can be written as

$$E[n(\mathbf{r})] = \sum_i f(\mu - \epsilon_i)\epsilon_i + F[n(\mathbf{r})], \tag{1}$$

where the first term is the band-structure energy. In a self-consistent calculation the eigenvalues $\epsilon_i$ and charge density $n(\mathbf{r})$ are determined self-consistently via the Kohn-Sham equations,[10] $\mu$ is the chemical potential, $f(\mu-\epsilon_i)$ is the Fermi function, and the sum is over all electronic states of the system. The function $F[n(\mathbf{r})]$ contains the remaining part of the DFT total energy: the ion-ion interaction energy, the parts of the Hartree and exchange-correlations not included in the eigenvalue sums, and the corrections for double counting in the eigenvalue sums. In an earlier TB model the electronic band-structure energy was determined from a parametrized Hamiltonian, and the remaining function $F[n(\mathbf{r})]$ was parametrized by a pair potential method. Based on the fact that the DFT allows an arbitrary shift in the potential without changes of total energy, Mehl *et al.*[4] developed an alternative TB method. By the shift Mehl *et al.*[4] transformed Eq. (1) into

$$E[n(\mathbf{r})] = \sum_i f(\mu' - \epsilon_i')\epsilon_i'. \tag{2}$$

Such a tight-binding method may solve the total-energy problem of Eq. (2), instead of Eq. (1), and does not need to

 

use an additional term, such as a pair potential term.

Mehl *et al.*[4] further simplified the problem by the two-center Slater-Koster formulation[11] with a nonorthogonal basis. The $\Sigma_i f(\mu' - \epsilon_i')\epsilon_i'$ consists of three terms: the on-site term, the Hamiltonian term, and the overlap term. All the three terms[4] have been given an analytical formula and parametrized by Mehl *et al*. The on-site term represents the energy required to place an electron in a specific orbital and depends on the local environment. The Hamiltonian term represents the matrix elements for electrons hopping from one site to another, and the overlap term describes the mixing between the nonorthogonal orbitals on neighbor sites. The eigenvalues $\epsilon'$ can be determined once these terms are evaluated for a given structure.

Finally, the potential parameters are determined by requiring that tight-binding method to reproduce first-principles total energies and electronic band structures of a real system.[4] This method has demonstrated the reliability in the calculations of structural behavior, elastic constants, phonon frequencies, vacancy formation energies, and surface energies of fcc metals.[4,5] In this work, we use the TB potential to study the stacking fault of Al, Pd, Pt, Ir, and Rh. The potential parameters of these metals are obtained from the web site http://cst-www.nrl.navy.mil/bind/; the program used in this work is the static version 111 from Mehl. Since the code cannot be used to carry out calculations of atom relaxation. We have revised it and added a simulated annealing code to the program.

## III. GENERALIZED STACKING-FAULT STRUCTURES AND ENERGIES

We model $\langle 112\rangle$ slip on a $(11\bar{1})$ slip plane for Al, Pd, Pt, Ir, and Rh by constructing a supercell that consists of 12 close-packed $(11\bar{1})$ planes of atoms. One atom in each plane is part of the supercell. The primitive vectors of the supercell take the form[5] of

$$\mathbf{a}_1 = \tfrac{1}{2}a_0\vec{y} + \tfrac{1}{2}a_0\vec{z},$$

$$\mathbf{a}_2 = \tfrac{1}{2}a_0\vec{x} + \tfrac{1}{2}a_0\vec{z},$$

$$\mathbf{a}_3 = \left(4 + \frac{q}{6}\right)a_0\vec{x} + \left(4 + \frac{q}{6}\right)a_0\vec{y} - \left(4 - \frac{q}{3}\right)a_0\vec{z}, \qquad (3)$$

where $a_0$ is the lattice constant, $q$ represents the stacking-fault variable, which is the displacement of atoms in the boundary plane along $\langle 112\rangle$ direction. When $q=0$ the periodic crystal is a perfect fcc system of $ABC|ABC$, where $|$ denotes a "boundary plane." When $q=1$, the atoms at the interface are hcp ordered, i.e., the stacking at the interface is $ABC|BCA$ rather than $ABC|ABC$. In this calculation the atoms in the three nearest atom layers to either side of the boundary plane are allowed to relax along the direction of $\langle 111\rangle$. We define the first interlayer spacing as the spacing between two atom layers nearest to the boundary plane. The two atom layers are located at either side of the boundary plane. The second interlayer spacing is defined as the spacing between the atom layers first and second nearest to the boundary plane. The atoms in the two atom layers are located on the same side of the boundary plane. Similar to the definition of the second interlayer spacing, the third interlayer spacing is the spacing between the atom layers second and third nearest to the boundary plane.

TABLE I. SFE and unstable SFE for Al, Pd, Pt, Ir, and Rh.

| Energy (mJ $m^{-2}$) | Al | Pd | Pt | Ir | Rh |
|---|---|---|---|---|---|
| SFE (this work) | 78 | 220 | 330 | 524 | 364 |
| (Expt.)[b] | 166 | 180 | 322 | 480 | 750 |
| (*Ab initio*)[b] | 150[a] | 161, 225 | 393 | 534 | 308, 320 |
| Unstable SFE (this work) | 178 | 374 | 422 | 637 | 606 |

[a]Ref. 12
[b]Ref. 16

To set up simulated annealing, first, at an initial temperature of 50 K, the program is run for 1000 steps. Then, the temperature is dropped to zero and the program is run for another 1000 steps. It should be noted that the primitive vectors of the supercell is determined by $q$. This means that once $q$ is given the shape and size of the cell cannot be changed during the process of simulated annealing. However, in order to eliminate the effect of a fixed height of the cell on the simulated results, we modified the code so that the cell height ($\mathbf{a}_3$) may be changed by the same small amount along $\vec{x}$, $\vec{y}$, and $-\vec{z}$, respectively.

The tight-binding method is very efficient computationally. A large number of $k$ points, 4808 in the irreducible part of the Brillouin zone of Eq. (3) have been used to ensure convergence. It is equivalent to using a mesh of 1202 $k$ points in the irreducible Brillouin zone of a fcc lattice. The total energy is determined by summing the eigenvalues with a weight of Fermi distribution over the first Brillouin zone of the lattice. We calculated SFEs and unstable SFEs for metals Al, Pd, Pt, Ir, and Rh. The relaxed SFEs and relaxed unstable SFEs, together with the results from the first-principles calculations and experiments are listed in Table I. From the table, it is seen that for SFEs of Pd, Pt, and Ir, a good agreement is found among our numerical results, experimental data, *ab initio* calculations. For SFE of Rh, although our numerical result is close to first-principles calculations, it is only about a half of experimental value in magnitude. In our calculations the SFE of Al is also found to be about a half of both experimental data and first-principles calculations. For unstable SFEs the present relaxed results are found to be in agreement with first-principles calculations for Al, and it is slightly larger than first-principles calculations for Pd.[12] In general, as shown in Table I, the present numerical results about the SFEs and unstable SFEs are comparable well with *ab initio* calculations and experiments for these metals. However, it is somewhat different from the results given by Mehl *et al.*[5] The difference, maybe, comes from the size effect of unit cell. In the calculations by Mehl *et al.* the supercell consists of nine atom layers while in the present calculations the cell consists of 12 atom layers.

The variations of the GSF energy versus stacking-fault variable $q$ and interlayer spacing versus $q$ are also calculated.

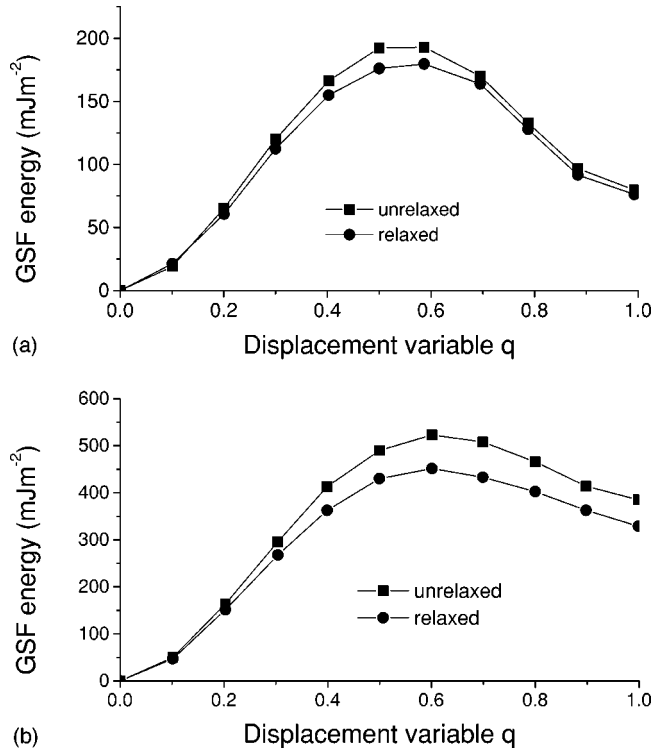


FIG. 1. GSF energy as a function of parameter $q$ in Eq. (3): (a) for Al and (b) for Pt. The lines are guides for the eyes.

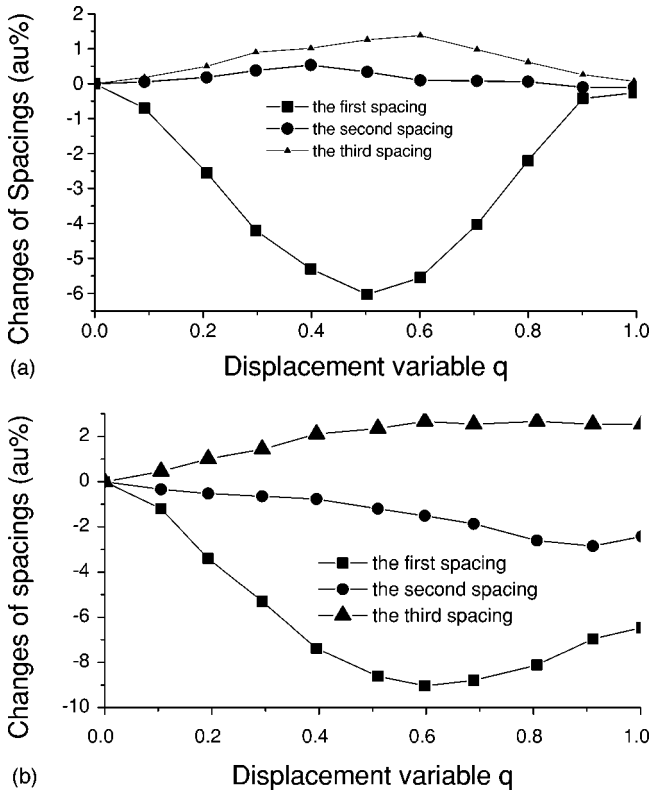


FIG. 2. The changes of interlayer spacings as a function of parameter $q$ in Eq. (3): (a) for Al and (b) for Pt.

The results of Al and Pt are shown in Figs. 1 and 2, respectively. Since metals Pd, Ir, and Rh have the similar curve shape to Al, the results are not shown here. Figure 1(a) is the curves of unrelaxed and relaxed GSF energy versus displacement $q$ for metal Al, and Fig. 1(b) for Pt. From the figures it is seen that the two curves have skewed sinusoidal shape. This is in agreement with the predictions by Frenkel,[13] Mackenzie,[14] and Rice.[15] In the present numerical calculations such a curve shape is also detected for Pd, Ir, and Rh. The present results are also in agreement with first-principles calculations,[3] where the GSF energy curves of Al, Cu, Ni, and Pd were found to have the skewed sinusoidal shape. But, the GSF energy curve shape of Al (Ref. 3) from the embedded-atom method is different from first-principles results.

It is interesting to note the peak position of the GSF energy curve. The peak corresponds to the unstable SFE. For the unrelaxed GSF energy curves of Al, Pd, Pt, and Ir, the peaks are found to locate at $q=0.54$, 0.56, 0.57, 0.54, and 0.55, respectively. For the corresponding relaxed GSF energy curves, the peaks are at $q=0.57$, 0.58, 0.6, 0.57, 0.58, respectively. [The results of Al and Pt are shown in Figs. 1(a) and 1(b).] All of the $q$s corresponding to the peaks are larger than 0.5. Previous first-principles calculations by Hartford[12] gave the $q$ value of 0.5 for Cu, 0.6 for Al, Pd, and Ni in a relaxed case. In an unrelaxed case Hartford[12] gave the values of 0.6 for Pd and Al. In addition, the calculations by van Schilfgaarde[3] gave the $q$ value greater than 0.5 for Ni. Hence in first-principles calculations except for Cu, the values of $q$s corresponding to the peaks on the GSF energy curve are larger than 0.5. This is in agreement with the present TB calculations. It is different from geometrical considerations, where the peak on GSF energy curve is at $q=1/2$ exactly.[3]

From Figs. 1(a) and 2(a) we also find that for Al the effect of atom relaxation on unstable SFE is larger than on SFE, i.e., the unstable SFE is reduced more than the SFE by atom relaxation. The conclusion is also true for Pd, Ir, and Rh. But for Pt, from Figs. 1(b) and 2(b), it is seen that the effect of atom relaxation on the SFE and the unstable SFE is almost the same. From the present numerical results it is seen that, with atom relaxation, the SFE is reduced by 1%, 7%, 14%, 3%, and 3%, while the unstable SFE is reduced by 7%, 17%, 14%, 23%, and 22% for Al, Pd, Pt, Ir, and Rh, respectively. In previous calculations for Ag and Au, it was also found that the SFEs were reduced by 1% and 6%, and the unstable SFEs were reduced over 10% and 20%, respectively, due to atom relaxation.[17] Thus, the effect of atom relaxation on SFE is far smaller than that on unstable SFE for Al, Pd, Ir, Rh, as well as Au and Ag, whereas the effect is large on both SFE and unstable SFE for metal Pt. This is an interesting result. In early calculations for SFEs, atomic relaxation was often neglected because the effect of atom relaxation on SFE was considered negligible. From present numerical calculations, it is seen that for most metals the effect of the relaxation on SFE is found to be small, while for Pt, this effect is very obvious on both SFE and unstable SFE. Thus, in order to calculate accurately SFE and unstable SFE, it is necessary to consider the effect of atom relaxation on SFE and unstable SFE, especially for an alloy system where the radii difference between two constituting elements is large.

Figure 2(a) shows the changes of atom layer spacings in Al due to atom relaxation. It can be seen that for Al the first

interlayer spacing has the largest change and contracts within the whole range of $q$ considered, while the third interlayer spacing expands. The second interlayer spacing expands initially and then contracts. The largest relaxation occurs at the place of unstable SFE. The first interlayer spacing has the largest relaxation. For Pd, Ir, and Rh, similar tendencies are also observed. In previous calculations by the authors for Au and Ag similar conclusions have also been drawn[17]. However, it is a different situation for metal Pt. From Fig. 2(b) it can be seen that in Pt the first and third interlayer spacings change similarly to those in Al, Pd, Ir, Rh, Au, and Ag, while the second interlayer spacing contracts in the whole range of $q$ considered. Unlike in metals Al, Pd, Ir, Rh, Au, and Ag, a large relaxation also occurs at the place of SFE in Pt for the three spacings. This corresponds to an obvious decrease in SFE of Pt due to atom relaxation. In addition, from the present numerical results it is also found that for metals Al, Pd, Pt, Rh, and Ir in the site of stacking fault ($q=1$) the interface structure is hcp-like. The calculated $c/a$ values are 1.624, 1.630, 1.622, 1.628, and 1.621, respectively. They are smaller than the ideal value of 1.633. These results are helpful for further testing of the accuracy of the potential model.

## IV. CONCLUSIONS

We use the TB potential of Mehl *et al.* to study the GSF of Al, Pd, Pt, Ir, and Rh. The potential predicts the properties of the GSF very well. First, the calculated SFEs for Pd, Pt, Ir, and Rh are in agreement with experimental values and first-principles calculations although for Al the value is about a half of experimental value. The predictions for skewed sinusoidal shape of the GSF energy versus displacement variable $q$ agree with the theoretical results by Freckle, Mackle, and Rice and *ab initio* calculations.[3] The site of unstable SFEs of Al, Pd, Pt, Ir, and Rh is found to be larger than the ideal value of $q=1/2$ from geometrical considerations. This property is in agreement with first-principles calculations.[3] More importantly, it is observed that although the effect of atom relaxation on SFE is small for metals Al, Pd, Ir, and Rh, the atom relaxation leads to a large change of SFE in Pt. Thus, it is concluded that in order to calculate accurately SFE and unstable SFE, it is necessary to consider atom relaxation, especially for an alloy system where the radii difference between two constituting elements is large.

## ACKNOWLEDGMENTS

C.J. thanks Professor Michael J. Mehl at the Naval Research Laboratory, Washington, D.C., for providing the TB program of static version 111.

[1] M. S. Daw and M. I. Baskes, Phys. Rev. B **29**, 6443 (1984); M. I. Baskes, *ibid.* **46**, 2727 (1992); R. A. Johnson, *ibid.* **41**, 9717 (1990); S. M. Foiles, M. I. Baskes, and M. S. Daw, *ibid.* **33**, 7983 (1986); J. Cai and Y. Y. Ye, *ibid.* **54**, 8398 (1996); **64**, 035402 (2001); A. Voter and S. P. Chen, Mater. Res. Soc. Symp. Proc. **82**, 175 (1987).

[2] J. Cai, Phys. Status Solidi B **203**, 345 (1997).

[3] J. A. Zimmerman, H. Gao, and F. F. Abraham, Modell. Simul. Mater. Sci. Eng. **8**, 103 (2000).

[4] M. J. Mehl and D. A. Papaconstantopoulos, Phys. Rev. B **54**, 4519 (1996).

[5] M. J. Mehl, D. A. Papaconstantopoulos, N. Kioussis, and M. Herbranson, Phys. Rev. B **61**, 4894 (2000).

[6] D. L. Medlin, S. M. Foiles, and D. Cohen, Acta Mater. **49**, 3689 (2001).

[7] M. A. Meyers, O. Vohringer, and V. A. Lubarda, Acta Mater. **49**, 4025 (2001).

[8] J. Cai, D. S. Wang, S. J. Liu, S. Q. Duan, and B. K. Ma, Phys. Rev. B **60**, 15 691 (1999).

[9] W. H. Press, S. A. Teukolsky, W. T. Vetterling, and B. P. Flannery, *Numerical Recipes in Fortran 77: The Art of Scientific Computing*, 2 ed., Vol. 1 Fortran Numerical Recipes (Cambridge University Press, Cambridge, 1997), p. 443.

[10] P. Hohenberg and W. Kohn, Phys. Rev. **136**, B864 (1964); W. Kohn and L. J. Sham, Phys. Rev. **140**, A1133 (1965).

[11] J. C. Slater and G. F. Koster, Phys. Rev. **94**, 1498 (1954).

[12] J. Hartford, B. von Sydow, G. Wahnstrom, and B. I. Lundqvist, Phys. Rev. B **58**, 2487 (1998).

[13] J. Frenkel, Z. Phys. **37**, 572 (1926).

[14] J. K. Mackenzie, PhD thesis, Bristol University, UK, 1949.

[15] J. R. Rice, J. Mech. Phys. Solids **40**, 239 (1992).

[16] N. M. Rosengaard and H. L. Skriver, Phys. Rev. B **47**, 12 865 (1993).

[17] J. Cai and J.-S. Wang, Eur. Phys. J. B **28**, 45 (2002); Modell. Simul. Mater. Sci. Eng. **10**, 469 (2002); J. Cai, C. Lu, P. H. Yap, and Y. Y. Wang, Appl. Phys. Lett. **81**, 3453 (2002).